

Spin-wave excitations and the magnetic phase transition in the ytterbium monopnictide YbAs

This article has been downloaded from IOPscience. Please scroll down to see the full text article.

1992 J. Phys.: Condens. Matter 4 4283

(<http://iopscience.iop.org/0953-8984/4/17/007>)

View [the table of contents for this issue](#), or go to the [journal homepage](#) for more

Download details:

IP Address: 171.66.16.96

The article was downloaded on 11/05/2010 at 00:12

Please note that [terms and conditions apply](#).

Spin-wave excitations and the magnetic phase transition in the ytterbium monopnictide YbAs

A Dönni^{||}, A Furrer[†], P Fischer[†], F Hulliger[‡] and S M Hayden^{§¶}

[†] Laboratory for Neutron Scattering, ETH Zürich, CH-5232 Villigen PSI, Switzerland

[‡] Laboratory for Solid State Physics, ETH Zürich, CH-8093 Zürich, Switzerland

[§] Institut Laue-Langevin, F-38042 Grenoble, France

Received 13 November 1991, in final form 17 January 1992

Abstract. Low-temperature neutron scattering experiments have been performed to investigate spin-wave excitations and the magnetic phase transition in the Kondo compound YbAs. In agreement with previous Mössbauer and specific heat experiments the present neutron results suggest that YbAs undergoes a first-order magnetic phase transition, which is smeared out in the crystal in an unusually large temperature range between 0.48 and 0.65 K. The spin-wave dispersion determined by bilinear magnetic exchange interactions is much stronger than the observed molecular-field splitting Δ_{MF} . This indicates that due to Kondo hybridization in YbAs the onset of long-range magnetic ordering is strongly suppressed and shifted to lower temperature. The mean-field spin-wave model for localized 4f electron systems which was appropriate to describe the magnetism of the dense Kondo systems CeAs and CeSe fails to describe the magnetism in YbAs. This result is not surprising because of the strong reduction of the observed magnetic moment of YbAs with respect to the crystal-field expectation value.

1. Introduction

With respect to Kondo hybridization, the monopnictides of the heavy rare earth Yb have attracted considerable interest in recent years [1]. For YbN, YbP and YbAs specific heat anomalies [2] indicated cooperative phase transitions to a magnetically ordered ground state in the temperature range below 1 K. From band-structure calculations [3] the excess specific heat peak observed in all three compounds around 5 K was attributed to the Kondo effect for a ground-state doublet. Mössbauer measurements [4] yielded magnetic saturation moments in YbP, YbAs and YbSb significantly reduced below the value $1.33 \mu_B$ expected from the crystal-field ground-state doublet Γ_6 , which is presumably due to Kondo hybridization. The electrical resistivity measured in YbP and YbAs [5] turned out to be only weakly sensitive to the magnetic phase transition. Transport properties are dominated by electrons, whereas measurements of the thermoelectric power [5] indicated the Kondo effect to be mainly due to holes.

Neutron diffraction experiments performed over the whole series of rocksalt-type ytterbium monopnictides YbX (X = N, P, As, Sb) confirmed the magnetic origin of

^{||} Present address: Department of Physics, Faculty of Science, Tohoku University, Sendai 980, Japan.

[¶] Present address: H H Wills Physics Laboratory, University of Bristol, Bristol, UK.

the specific heat anomalies [2]. Stoichiometric compounds of YbN [6] and YbAs [7, 8] exhibit long-range antiferromagnetic ordering of type III, corresponding to $k = [1, 0, \frac{1}{2}]$ below $T_N = 0.79$ K and $T_N \simeq 0.7$ K, respectively. The low magnetic saturation moments of $0.39 \mu_B$ (YbN) and $0.86 \mu_B$ (YbAs) are oriented perpendicular to the c axis of the tetragonal magnetic unit cell. An ytterbium phosphide sample with a non-stoichiometric composition of YbP_{0.84} [9] showed long-range antiferromagnetic ordering of type II, corresponding to $k = [\frac{1}{2}, \frac{1}{2}, \frac{1}{2}]$ below $T_N = 0.64$ K with the magnetic moments ($1.03 \mu_B$ at saturation) perpendicular to the propagation vector. In contrast to the interpretation of previous Mössbauer data [4] neutron diffraction experiments performed in stoichiometric YbSb [10] indicated the absence of long-range magnetic ordering down to 7 mK. Defects due to non-stoichiometry and inhomogeneity may significantly influence the physical properties in the ytterbium monopnictides, and this is the reason for the contradictory results obtained for different samples, especially of YbP [2, 9, 11].

In a previous investigation [7] we determined the magnetic structure of YbAs using a single crystal of volume 150 mm^3 . For the work reported here we used the same large YbAs single crystal as in [7] and continued the neutron scattering experiments in order to study the unusual magnetic phase transition of YbAs in more detail, as well as to measure spin-wave excitations in the magnetically ordered state. The results of these experiments are summarized in section 3 and discussed in section 4.

A measurement of the spin-wave dispersion by inelastic neutron scattering can provide a very detailed picture of magnetic interactions on a microscopic level. Such experiments have been performed for the rocksalt-type dense Kondo compounds CeAs [12] and CeSe [13]. In the data analysis the influence of Kondo hybridization on the well isolated crystal-field ground-state doublet was neglected, and anisotropic magnetic interactions between fully localized 4f electrons of the magnetic Ce³⁺ ions were phenomenologically described via a model Hamiltonian in a generalized Heisenberg form. Using the Green's function formalism in the random-phase approximation a self-consistent effective spin- $\frac{1}{2}$ mean-field Hamiltonian with highly anisotropic bilinear nearest-neighbour exchange interaction was appropriate to describe the experimentally observed magnetic properties in both systems, CeAs and CeSe.

This theoretical spin-wave model can be adapted to the FCC type-III antiferromagnetic structure of YbAs. The resulting expressions for calculating spin-wave excitation energies and intensities as functions of tetragonal anisotropic bilinear magnetic exchange interactions are given in [13]. The experimentally observed spin-wave excitation spectra in the present work provide evidence that this mean-field formalism for fully localized 4f electrons is inappropriate for describing the magnetic properties of YbAs, where the influence of Kondo hybridization on the well isolated crystal-field ground-state doublet Γ_6 cannot be neglected. At present the appropriate form of the Hamiltonian including the effect of Kondo hybridization is not clear.

This result is supported by specific heat experiments. For both CeAs [14] and CeSe [15] the specific heat anomaly at the magnetic phase transition contains a magnetic entropy close to the value of $R \ln 2 = 5.76 \text{ J mol}^{-1} \text{ K}^{-1}$, the molar entropy expected for a ground-state doublet. This is in contrast to the results for the ytterbium monopnictides YbN, YbP and YbAs, where the cooperative magnetic phase transitions below 1 K only release about 20% of the expected value $R \ln 2$ [2]. The total entropy $R \ln 2$ is only recovered if the temperature is raised to much above 10 K, i.e., more than an order of magnitude above the magnetic ordering

temperatures.

2. Sample preparation and experimental details

The YbAs sample was obtained in a two-step process. The first step comprised the prereaction. Fine turnings of 3N Yb (Research Chemicals, Phoenix, AZ), prepared under flowing argon from a one-inch bar, were reacted with 4N As in closed evacuated quartz ampoules. The ampoules were slowly heated up to about 600 °C and kept at this temperature until the reaction appeared to be completed. In order to homogenize the samples the ampoules were heated to 800 °C for another day. For the second step the resulting greyish powder (20 g) was pressed into pellets of 12.5 mm diameter and filled into a tungsten crucible (total height \approx 30 mm). The sealed crucible was heated to above the melting point of YbAs, slowly cooled to about 50–100 °C below this temperature, and after 10 days cooled to room temperature. The resulting ingot turned out to consist of large single-crystal domains. The room temperature lattice constant of $a_{295\text{ K}} = 5.6957(9)$ Å for YbAs was determined by x-ray diffraction with a Guinier–Jagodzinski camera from Cu $K\alpha_1$ radiation and with silicon as the internal standard (assuming $a = 5.43047$ Å at 295 K).

The magnetic phase transition has been studied by neutron diffraction experiments performed on the double-axis spectrometer at the reactor Saphir (Würenlingen). The neutron wavelength $\lambda = 2.337$ Å was obtained from a graphite (0,0,2) monochromator. A pyrolytic graphite filter 120 mm thick was inserted in the monochromatic beam to eliminate higher-order contamination. The crystal clamped with a vertical [0,0,1] axis to a copper sample holder was mounted in a He(3,4) dilution refrigerator reaching 7 mK as the lowest temperature.

Spin-wave excitations in the ordered state of YbAs were studied in an inelastic neutron scattering experiment on spectrometer IN12 at the cold source at ILL, Grenoble. The single crystal of YbAs was mounted with a (0,0,1) orientation in a dilution refrigerator. Measurements were performed at 200 mK with a collimation of $60^\circ/60^\circ/60^\circ$ from monochromator to detector. The incoming neutron energy was kept fixed at 2.28, 2.51, 3.24, 4.06 and 4.66 meV, which yields instrumental resolutions ($\Delta E = 0$) of 0.04, 0.05, 0.09, 0.14 and 0.18 meV, respectively.

3. Results

3.1. The magnetic phase transition

The magnetic Bragg peaks detected in YbAs at 7 mK correspond to FCC antiferromagnetic ordering of type III with ordering wave vector $k = [1, 0, \frac{1}{2}]$ as reported in [7]. In the magnetic Z domain (consisting of the eight propagation vectors $[1, 0, \pm \frac{1}{2}]$, $[-1, 0, \pm \frac{1}{2}]$, $[0, 1, \pm \frac{1}{2}]$ and $[0, -1, \pm \frac{1}{2}]$) the magnetic unit cell is doubled along the z axis as compared with the nuclear FCC cell, illustrated in figure 1. The $[1, 0, \frac{1}{2}]$ domain shown in figure 1 consists of a superposition of a (+−) stacking along x , a (+) stacking along y and a (+ + − −) stacking along z . From neutron diffraction data obtained on a magnetic multidomain single crystal a determination of the explicit direction of the magnetic moments perpendicular to the z axis of the tetragonal magnetic cell is

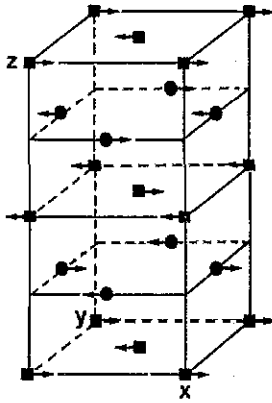


Figure 1. FCC antiferromagnetic type-III structure of YbAs corresponding to $\mathbf{k} = [1, 0, \frac{1}{2}]$ with ferromagnetic coupling between the two sublattices ■ and ●. (Antiferromagnetic coupling corresponds to $\mathbf{k} = [1, 0, -\frac{1}{2}]$.)

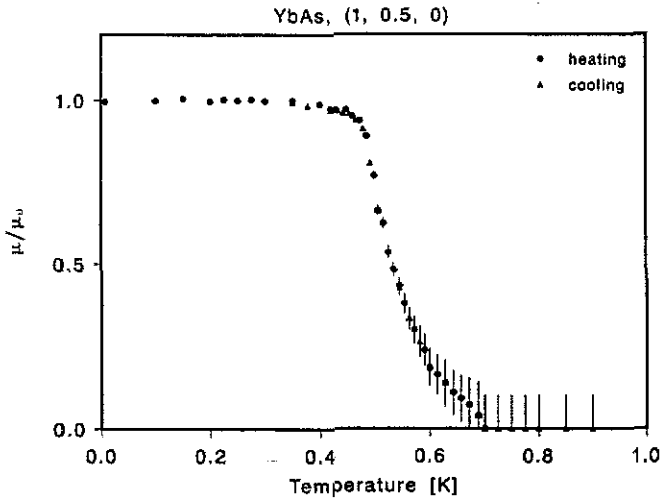


Figure 2. Temperature dependence of the average reduced ordered magnetic moment μ/μ_0 per Yb^{3+} ion of YbAs derived from the magnetic peak $(1, \frac{1}{2}, 0)$. According to the Mössbauer results magnetically ordered and paramagnetic domains coexist between 0.48 and 0.65 K.

not possible. For the case plotted in figure 1 the ordered moments $g\mu_B \langle S^x \rangle$ at the lattice sites R_i are given by

$$\langle S_i^x \rangle = \frac{1}{2} [(1 - i)e^{iq_0 \cdot R_i} + (1 + i)e^{-iq_0 \cdot R_i}] \langle S^x \rangle \quad (1)$$

with the ordering vector $q_0 = (2\pi/a)(1, 0, \frac{1}{2})$.

The temperature dependence of the average sublattice magnetization, determined as the square root of the magnetic peak intensity of the reflection $(1, 0, \frac{1}{2})$, is shown in figure 2. The thermal variation is rather unusual: the average magnetic moment remains almost constant up to 480 mK, where it suddenly drops (93%, 84%, 68%, 60% and 50% at 480, 490, 500, 510 and 520 mK, respectively), but the final decrease towards the Néel temperature is rather slow (38%, 18%, 8% and 0% at 550, 600, 650 and 700 mK, respectively). With a temperature stability better than 5 mK the experiments yield no hysteresis. The magnetization curves obtained from the peaks $(1, 0, \frac{1}{2})$

and $(1,0,\frac{3}{2})$ are practically identical [7], so a temperature-dependent reorientation of the magnetic moment can be excluded. Scans along $(q,0,0)$ and $(0,q,0)$ through the magnetic peak $(1,\frac{1}{2},0)$ at different temperatures are shown in figure 3. No critical scattering and no temperature dependence of position and half-width of the magnetic Bragg peak $(1,\frac{1}{2},0)$ was observed, so there is long-range magnetic ordering up to $T_N \simeq 0.65$ K.

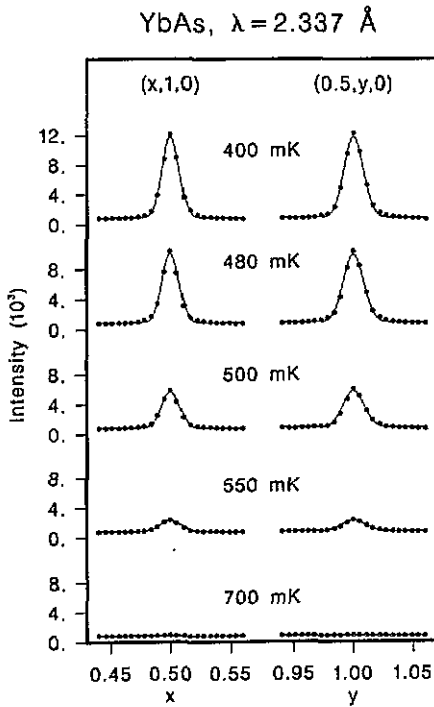


Figure 3. Scans along $(q,0,0)$ and $(0,q,0)$ through the magnetic peak $(\frac{1}{2},1,0)$ of YbAs at different temperatures.

3.2. Spin-wave excitations

Magnetic multidomain spin-wave excitation spectra of YbAs along the $[\xi, 0.5, 0]$ direction are shown in figure 4. Although contributions from the 24 different magnetic domains give rise to 12 or 24 different excitations (for the cases of isotropic or anisotropic bilinear magnetic coupling, respectively, see [13]), the observed spectra (figure 4) basically consist of two different excitation groups. One group has a constant excitation energy of 0.31 meV, as plotted in figure 5, whereas the other group exhibits a strong dispersion with an energy gap of 0.08(2) meV at the W point, and excitation energies above 0.6 meV at $Q = (0.7, 0.5, 0)$. In the vicinity of $Q = (1, 0.5, 0)$ the dispersions measured along the directions $[\xi, 0.5, 0]$ (shown in figure 5) and $(1, \xi, 0)$ (not shown) look quite similar. At the magnetic zone centre $Q = (1, 0.5, 0)$, the intensities of the excitations exhibit a strong maximum and drastically decrease with distance from the W point. Because of the weak intensity of the excitations and the necessarily good instrumental energy resolution, the spin-wave excitations could only be observed in the vicinity of the magnetic zone centres. The different polarizations of the excitations of the two groups of figure 5 are illustrated in figure 6, which

contains the spectra measured at $Q = (0.95, 0.5, 0)$ and at $Q = (0.95, 1.5, 0)$. The temperature dependence of the spin-wave excitations of YbAs measured at $Q = (0.9, 0.5, 0)$ is shown in figure 7.

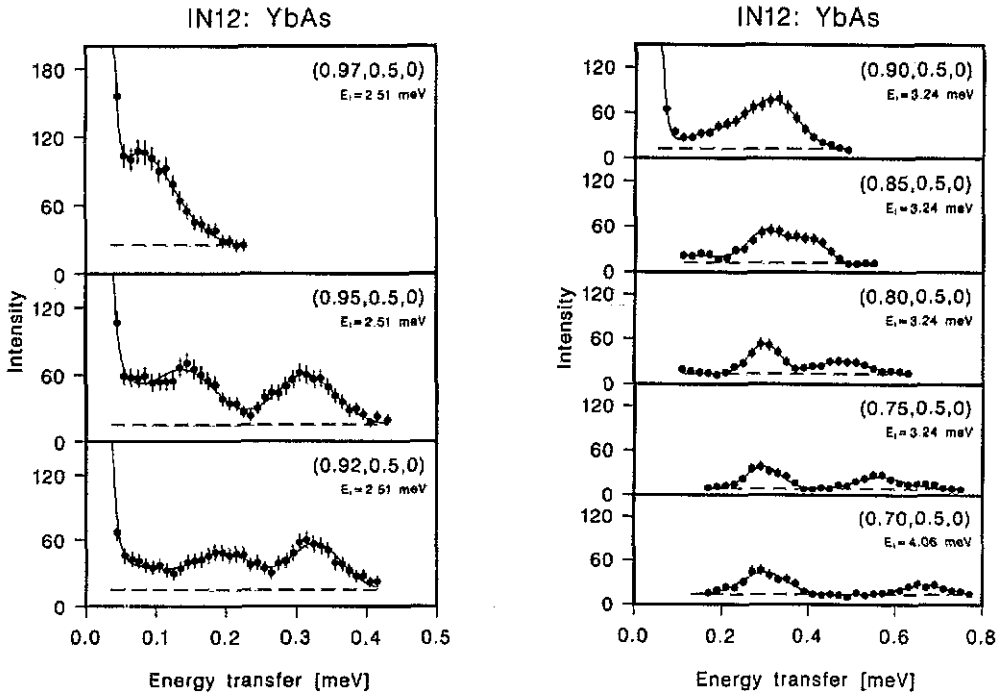


Figure 4. IN12 multidomain spectra of YbAs along the $(\xi, 0.5, 0)$ direction measured at 0.20 K with constant incoming energies $E_i = 2.51$ meV, $E_i = 3.24$ meV and $E_i = 4.06$ meV. Solid lines are guides to the eye.

4. Discussion

4.1. The magnetic phase transition

The unusual temperature dependence of the average sublattice magnetization (figure 2) is in striking agreement with the results of previous Mössbauer experiments performed by Bonville *et al* [16]: in the Mössbauer spectra 50 mK (see figure 1 in [16]) the observed magnetic hyperfine structure (Zeeman quintet) indicates antiferromagnetic ordering. At 700 mK a single-line paramagnetic spectrum is observed. At 500 mK in the neighbourhood of the magnetic transition the observed lineshape consists of the superposition of the two spectra indicating a coexistence of a (magnetically saturated) antiferromagnetic fraction and a paramagnetic fraction at this temperature. The hyperfine field (H_{HF}) of the antiferromagnetic fraction, which is proportional to the Yb^{3+} 4f-shell magnetic moment, remains practically constant below T_N . The paramagnetic–antiferromagnetic transition does not occur through a progressive decrease to zero of the hyperfine field, but rather through a decrease in the proportion of the magnetically ordered fraction. The temperature dependence of

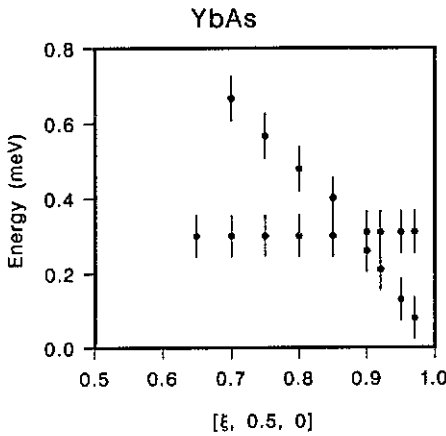


Figure 5. The observed multidomain spin-wave dispersion of YbAs along the $[\xi, 0.5, 0]$ direction. Vertical bars indicate the widths of the observed excitations.

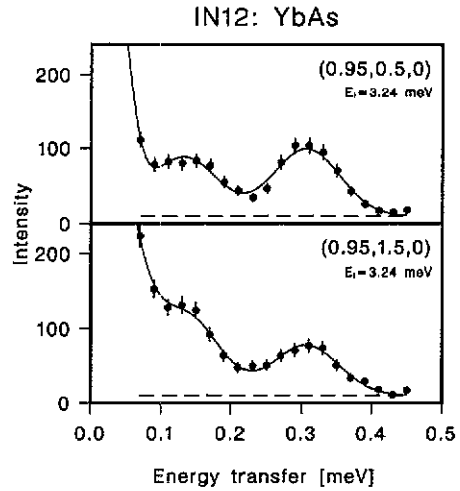


Figure 6. IN12 spectra of YbAs measured at $Q = (0.95, 0.5, 0)$ and $Q = (0.95, 1.5, 0)$ illustrating the different polarizations of the excitation groups. Solid lines are guides to the eye.

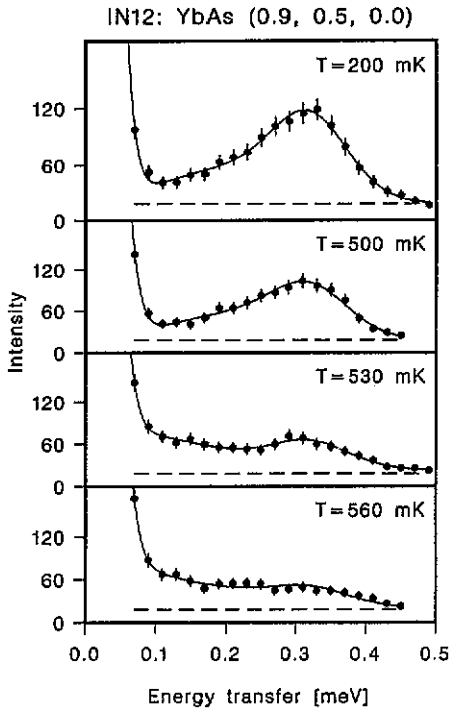


Figure 7. Temperature dependence of the magnetic excitations of YbAs at $(0.9, 0.5, 0)$. The IN12 spectra were measured with constant $E_i = 3.24$ meV. Solid lines are guides to the eye.

the relative proportion of the antiferromagnetic fraction obtained by Mössbauer spectroscopy [16] is practically identical with the temperature dependence of the average sublattice magnetization obtained by neutron diffraction (figure 2).

According to the Mössbauer results figure 2 actually reflects the progressive decrease of the overall volume of magnetically ordered domains as temperature increases and cannot be interpreted as a decrease of the Yb sublattice magnetization, which is independent of temperature below T_N . The magnetic phase transition in YbAs is of first order and smeared out in the crystal in a large temperature range of ≈ 0.17 K. According to figure 2, 50% of the crystal has transition temperatures between 480 mK and 520 mK in agreement with the specific heat anomaly [2], but up to $T_N \approx 0.65$ K a small fraction of the crystal exhibits long-range magnetic ordering.

The specific heat anomaly at the magnetic phase transition of YbAs measured by Oyamada *et al* [8] consists of a quite sharp lower-temperature side and an unusual tail extending to the higher-temperature side, which is in nice agreement with Mössbauer and neutron results. Additional neutron scattering experiments [8] also yielded antiferromagnetic type-III ordering in YbAs with the moments perpendicular to the c axis, absence of critical scattering and absence of hysteresis. For their YbAs sample with slightly lower transition temperatures a smaller saturation moment $\mu_{Yb} = 0.6 \mu_B$ was measured using a neutron wavelength $\lambda = 0.83 \text{ \AA}$. Between 500 mK and 530 mK a shift of the magnetic propagation vector from the commensurate value of $k = [1, 0, 0.5]$ to an incommensurate value of $k = [1, 0, 0.498]$ at higher temperatures was claimed [8], which is incompatible with the results of figure 3. Measurements of magnetic field dependence of the magnetic peak intensities revealed domain motions, which is typical for a single- k structure.

At present, the reason for this unusually large temperature range of coexistence of antiferromagnetic and paramagnetic phase in YbAs is not clear. This effect is sample independent in the sense that the results obtained for four different YbAs samples [2, 7, 8, 16] are in almost perfect agreement. The contradictory results obtained for different samples of YbN, YbP and YbSb indicate that, in the series of ytterbium monpnictides, so far the YbAs samples have the highest quality as regards stoichiometry and homogeneity. Similarly to what is observed for YbAs in CeAs, the second-order magnetic phase transition was found to be smeared out in the crystal in the large temperature range $7.5 \text{ K} < T < 8.5 \text{ K}$ [17]. In the case of CeAs this behaviour had been attributed to the existence of a nearly gapless spin-wave mode [12, 18].

4.2. Spin-wave excitations

We compare the spectra of YbAs (figures 4, 5) with the previously measured spin-wave spectra of CeAs (FCC type-I antiferromagnet, $k = [0, 0, 1]$; see [12]), CeSe (FCC type-II antiferromagnet, $k = [\frac{1}{2}, \frac{1}{2}, \frac{1}{2}]$; see [13]), and CeSb (FCC type-Ia antiferromagnet at $T = 4.2 \text{ K}$, $k = [0, 0, \frac{1}{2}]$; see [12]). The magnetic multidomain spectra of CeAs, CeSe and CeSb all look similar, containing two groups of excitations. At the magnetic zone centres (CeAs: X point; CeSe: L point) or the X point (CeSb) the two groups exhibit the maximal splitting in energy with the excitations corresponding to the dispersion minimum Δ_{gap} and to roughly the molecular-field splitting Δ_{MF} . Besides this low-energy branch reaching the energy gap Δ_{gap} , the total energy dispersion along the main symmetry directions of the nuclear lattice is rather small, being less than $\Delta_{\text{MF}}/2$.

The observed spectra of CeAs, CeSe and CeSb were all reproduced by calculations using the mean-field spin-wave theory for the appropriate magnetic structure. For all the compounds the bilinear nearest-neighbour coupling turned out to be highly anisotropic. Furthermore, in CeAs and CeSe a single magnetic domain exhibits the

energy gap excitation (Δ_{gap}) not at its own magnetic zone centre but at the magnetic zone centre of a different magnetic domain.

Using the results on CeAs, CeSe and CeSb in an interpretation of the multidomain spectra of YbAs (figures 4, 5), the dispersionless excitation group at 0.31 meV is expected to correspond to the molecular-field splitting Δ_{MF} . Similar to the cerium compounds, YbAs has multidomain spectra that contain a low-energy branch reaching the energy gap $\Delta_{\text{gap}} = 0.08$ meV at the magnetic zone centre. However, the contrast to the spin-wave spectra of the cerium compounds, the excitation group with the strong dispersion (figure 5) in YbAs reaches excitation energies of above twice the value of the molecular-field splitting Δ_{MF} at $Q = (0.7, 0.5, 0)$.

Within a mean-field spin-wave model for localized 4f electrons the wave-vector dependence of the spin-wave excitation energies $\omega(q)$ is determined by the Fourier-transformed bilinear exchange interactions $J(q)$ because the Γ_6 ground-state doublet of YbAs has no quadrupolar matrix elements. For vanishing $J(q) \equiv 0$ the dispersion becomes flat, corresponding to the molecular-field splitting $\Delta_{\text{MF}} = \Delta_J + \Delta_Q$, which contains contributions from bilinear interactions (Δ_J) and quadrupolar interactions (Δ_Q). The stability of the magnetic structure requires that for all wave vectors q

$$|\omega(q) - \Delta_{\text{MF}}| \leq \Delta_{\text{MF}}. \quad (2)$$

That is, the whole energy dispersion must be within the energy range from 0 to $2\Delta_{\text{MF}}$. Equation (2) is satisfied by the experimentally observed spin-wave dispersions in all the compounds CeAs, CeSe and CeSb. However, since the spin-wave dispersion of YbAs shown in figure 5 violates (2), the model can never explain the observed data. Compared with the observed molecular-field splitting Δ_{MF} in YbAs, the spin-wave dispersion determined by the bilinear magnetic exchange interactions turns out to be too large. Assuming that strong quadrupolar interactions are present in YbAs, the observed splitting $\Delta_{\text{MF}} = 0.31$ meV is possible for the observed magnetic ordering temperatures (between 0.48 K and 0.65 K). However, for the case of fully localized 4f electrons the observed bilinear exchange interactions of YbAs must lead to a much higher Néel temperature, possibly corresponding to the specific heat anomaly around 5 K. Due to Kondo hybridization in YbAs the onset of long-range magnetic ordering is strongly suppressed and shifted to lower temperatures.

Recently the low-temperature part of the specific heat of YbAs measured by Oyamada *et al* [8] was analysed by fitting a spin-wave dispersion with energy gap $E = Dk + \Delta$. Independently of the present work they obtained an energy gap of 3 K [19] roughly corresponding to the excitation energy $\Delta_{\text{MF}} = 0.31$ meV = 3.6 K of the spin-wave group with flat dispersion in figure 5.

The temperature dependence of the spin-wave excitations of YbAs is shown in figure 7. At $T \geq 0.5$ K in the coexistence range of magnetically ordered and paramagnetic regions in the crystal (see section 4.1) the excitations do not shift in energy, in agreement with a first-order phase transition. With increasing temperature the spin-wave excitations decrease in intensity, whereas the quasielastic scattering from the paramagnetic regions gains intensity.

Acknowledgments

We are indebted to Professor T Suzuki and Dr A Oyamada for stimulating discussions. Financial support from the Swiss National Science Foundation is gratefully acknowledged.

References

- [1] See e.g.
Bonville P 1988 *Hyperfine Interact.* **40** 15
- [2] Ott H R, Rudigier H and Hulliger F 1985 *Solid State Commun.* **55** 113
- [3] Monnier R, Degiorgi L and Delley B 1990 *Phys. Rev. B* **41** 573
- [4] Bonville P, Hodges J A, Hulliger F, Imbert P, Jéhanno G, Marimom da Cunha J B and Ott H R 1988 *J. Magn. Magn. Mater.* **76-7** 473
- [5] Oyamada A, Ayache C, Suzuki T, Rossat-Mignod J and Kasuya T 1990 *J. Magn. Magn. Mater.* **90-1** 443
- [6] Dönni A, Fischer P, Furrer A, Bacsá W and Wächter P 1990 *Z. Phys. B* **80** 269
- [7] Dönni A, Fischer P, Furrer A and Hulliger F 1989 *Solid State Commun.* **71** 365
- [8] Oyamada A, Burllet P, Bouvet A, Calemczuk R, Rossat-Mignod J, Suzuki T and Kasuya T 1990 *J. Magn. Magn. Mater.* **90-1** 441
- [9] Dönni A, Fischer P, Furrer A, Bonville P, Hulliger F and Ott H R 1990 *Z. Phys. B* **81** 83
- [10] Dönni A, Furrer A, Fischer P, Hulliger F, Wächter P and Ott H R 1990 *J. Magn. Magn. Mater.* **90-1** 143
- [11] Takagi S, Oyamada A and Kasuya T 1988 *J. Phys. Soc. Japan* **57** 1456
- [12] Hälgl B and Furrer A 1986 *Phys. Rev. B* **34** 6258
- [13] Dönni A 1991 *Dissertation 9403* ETH Zürich
- [14] Hulliger F and Ott H R 1978 *Z. Phys. B* **29** 47
- [15] Hulliger F, Natterer B and Ott H R 1978 *J. Magn. Magn. Mater.* **8** 87
- [16] Bonville P, Hodges J A, Hulliger F, Imbert P, Jéhanno G, Marimom da Cunha J B and Ott H R 1988 *Hyperfine Interact.* **40** 381
- [17] Hälgl B, Furrer A and Kjems J K 1987 *Phys. Rev. Lett.* **59** 1034
- [18] Prelovsek P and Rice T M 1987 *Phys. Rev. B* **59** 1248
- [19] Oyamada A, Suzuki T, Kasuya T, Calemczuk R, Burllet P and Rossat-Mignod J 1992 *J. Magn. Magn. Mater.* at press